

The influence of plasma on the morphological and structural properties of TiO₂ thin films

O. DURANTE⁽¹⁾⁽²⁾, J. NEILSON⁽²⁾⁽³⁾ and C. DI GIORGIO⁽¹⁾⁽²⁾

⁽¹⁾ *Department of Physics “E.R. Caianiello”, University of Salerno - Fisciano, Italy*

⁽²⁾ *INFN, Sezione di Napoli Gruppo Collegato di Salerno - Napoli, Italy*

⁽³⁾ *Department of Engineering, DING, University of Sannio - Benevento, Italy*

received 29 January 2022

Summary. — Uniform and dense titanium dioxide (TiO₂) thin films, required in several fields, can be achieved by using standard deposition. Here, we investigate the effect of using a plasma source during e-beam deposition on the morphological and structural properties of TiO₂ thin films. We show that morphology, crystallization onset temperature, and crystallization evolution are all affected by the change in material density, achieved by employing or not plasma bombardment.

1. – Introduction

The scientific interest in the study of titanium dioxide (TiO₂) thin films, both in the amorphous and crystalline forms (anatase, brookite, and rutile), arises from the large number of material applications in the field of electronics, photocatalysis, and optics. In this context, device optimization and development need a high control of TiO₂ properties like chemical stability, refractive index, and density. The latter, in particular, affects the material packing form and its crystallization dynamic, and can be controlled via deposition techniques, such as reactive evaporation, ion beam sputtering, and plasma-enhanced chemical vapor deposition [1]. In this work, we have used e-beam deposition at room temperature, for its versatility and wide use in producing thin films, and we have tuned the material uniformity and packing density, which ultimately affect the mechanical and optical properties of the thin films [2], by performing fabrication with and without ion-plasma bombardment assistance. Here, we then focused on the effect of plasma on the morphological and structural properties of TiO₂ thin films (as-grown, and after post-deposition annealing) through atomic force microscopy (AFM), X-ray diffraction (XRD), and Raman spectroscopy (RS).

2. – The influence of plasma: Results and discussion

Amorphous TiO₂ thin films, with a nominal thickness of 200 nm, were fabricated on (100) Si substrates by using an electron-beam evaporator. In order to study the influence of plasma bombardment on the morphological and structural properties of as-grown and annealed TiO₂ samples, two types of samples have been fabricated, without (NP) and with (WP) the assistance of a plasma source, made by the mixture of Ar and O₂. Figures 1(a), (b) show representative tapping-mode AFM morphologies, acquired on a scan area of 1 $\mu\text{m} \times 1 \mu\text{m}$, of the as-grown NP and WP samples, respectively. Noteworthy, the surface of both samples shows packed particles. These particles are typical features of amorphous growths due to room temperature deposition [3]. Amorphicity is further confirmed by the absence of crystalline peaks in the XRD and RS —magenta for NP and cyan curves for WP, in figs. 1(c), (d), respectively. By comparing panels (a) and (b), it can be deduced that the particle size for the two samples is different. The latter has

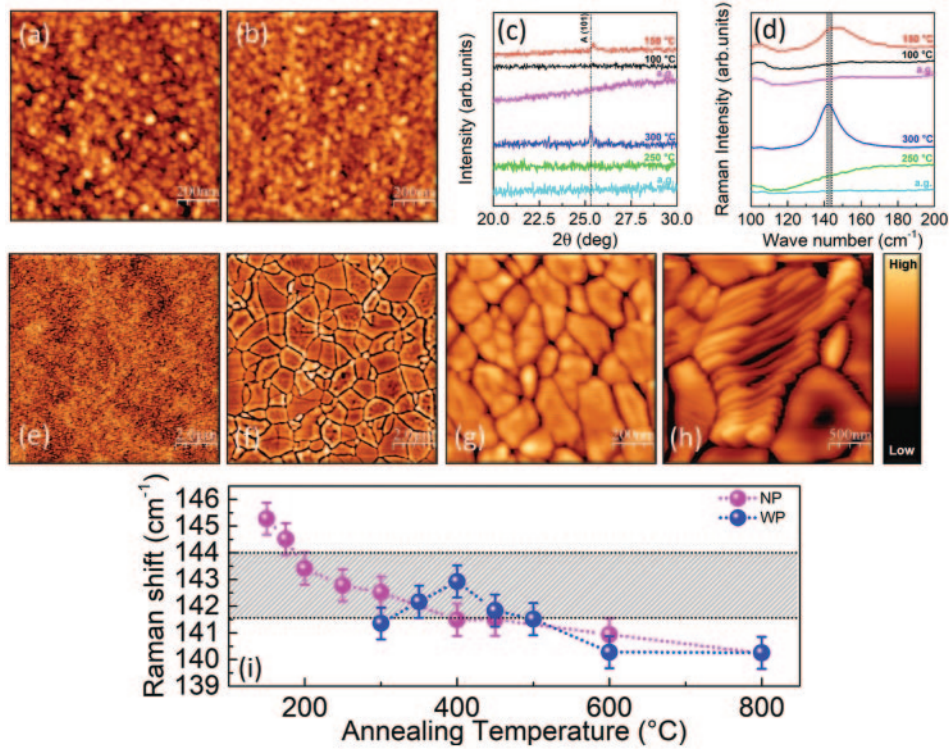


Fig. 1. – Tapping-mode AFM topography of as-grown ((a), (g)) NP (a) and WP (b) samples; (c) XRD spectra, and (d) RS spectra. The magenta (cyan), black (green), and red (blue) curves indicate the spectra for the NP (WP) sample, as-grown and annealed at 100 (250), and 150 (300) °C, respectively. Tapping mode AFM topography of NP (e, g), and of WP (f, h), annealed at 800 °C. The scan areas are 10 $\mu\text{m} \times 10 \mu\text{m}$ ((e), (f)), 1 $\mu\text{m} \times 1 \mu\text{m}$ (g), and 2.5 $\mu\text{m} \times 2.5 \mu\text{m}$ (h). The color scale for ((a), (b)) range from 0 to 5 nm, for (e) from 0 to 15 nm, for (f) from 0 to 50 nm, and for ((g), (h)) from 0 to 20 nm. (i) Raman shift as a function of the annealing temperature for the NP (magenta dots), and WP (blue dots) samples. Dashed lines used in (i) are guides for the eye.

been estimated by taking into account several factors, such as the convolution between the particles and the tip size, the high packing density, and the finite tip size. By using the approach discussed in ref. [4], we evaluated (44 ± 6) nm as the effective average size of particles for NP, and (37 ± 3) nm for those of WP. Thus, the particle size of NP is larger than that of WP, probably due to the fact that ions, during deposition, increase the homogeneous nucleation rate, which leads to a larger number of smaller particles in the sample [5]. Furthermore, the plasma influence on the surface morphology is also highlighted by the presence of many “voids”, *i.e.*, the dark areas in panels (a), (b), that are more evident in NP than in WP, thus confirming that a better packing is observed in WP. Besides proving the amorphicity of the samples, XRD and RS measurements were used to explore the amorphous-to-crystalline phase transition and to study the evolution of crystallization in both NP and WP samples. The annealing processes were carried out in air, for 12 h, in a temperature range of 150–800 °C separated by a minimum step of 50 °C. The black and red (green and blue) curves in

figs. 1(c), (d) show XRD and RS spectra of the NP (WP) sample, after annealing at 100 and 150 °C (250 and 300 °C), respectively. In panel (c), the black (100 °C) and green (250 °C) curves show no TiO_2 reflections, demonstrating that NP and WP are still amorphous at those temperatures. Instead, the red (150 °C) and blue (300 °C) curves show the strongest anatase reflection, A (101), at $2\theta = 25.2^\circ$ of TiO_2 , proving the onset of crystallization. The same situation is observed by RS in panel (d), where the strongest anatase Raman vibrational band, *i.e.*, the E_g mode at 144 cm^{-1} , is observed as the manifestation of crystallization. In this way, both XRD and RS analysis determine the crystallization onset temperature, which is 100–150 °C for NP and 250–300 °C for WP. We thus observe that WP shows a higher crystallization onset temperature than NP. This phenomenon can be attributed to the influence of plasma, which increases the density of material, giving rise to smaller particles with higher compactness. It has been indeed demonstrated that the crystallization temperature, as well as the melting one, increases as the particle size decreases [6]. Additionally, also the surface evolution in temperature is quite different for NP and WP. Panels (e)–(h) compare representative tapping mode AFM topographies acquired on a large (e), (f) and small (g), (h) scan area of NP and WP samples annealed at the highest temperature of 800 °C. Due to the high annealing temperature, the surface of both samples appears entirely cracked in plates or blocks, but their size and orientation appear different. Indeed, the surface of NP is formed by smaller grains compared to WP, which seem to be still not coalescing into larger blocks (panel (e)) as is the case of WP (panel (f)). On a smaller scan area, the surface of both NP and WP shows grains with different crystalline orientations, one from the other. These peculiar structures can depend on the degree of non-stoichiometry of the sample. Flat and smooth grains, as shown in panel (g), can indicate that stoichiometry is very close to the nominal one. On the contrary, grains with vertically developed “terraces” (central feature in panel (h)) can indicate an incorrect stoichiometry [7]. The stepped grain ridges observed in this panel can form in thin film materials, as a consequence of growth with plasma-assist and lattice mismatch between the film and the substrate. Finally, we have used RS to explore the effect of plasma on the structural properties on both TiO_2 samples by studying the E_g anatase Raman mode as a function of the annealing temperature. Figure 1(i) shows the E_g peak position as a function of the annealing temperature for NP (magenta dots) and WP (blue dots) samples, compared to the E_g reference values [8] (gray shaded region). As a consequence of crystallization, NP and WP show two different behaviors: a monotonic decrease of the E_g mode position is observed for NP, moving from wavenumbers that are blue-shifted, compared to the expected E_g , to a very tiny red-shift

at the highest temperature (from 400 to 800 °C). Conversely, the WP sample exhibits a wavenumber position of the Eg band scattered around the expected value (141.5 cm^{-1}), whereas a trend with a slight red shift is measured when the annealing temperature is 600 °C or higher. The blue shift at the beginning of crystallization can be related to the size of the so-formed anatase TiO_2 crystallites [9,10]. Indeed, in the approximation of spherical particles, the phonon is progressively confined within the nanocrystal, as its size decreases from 20 nm to 2 nm, producing a re-shaping of the correspondent vibrational band, whose peak results blue-shifted compared to the bulk value [11]. Moreover, the comparison between the value of the blue-shift measured in NP and the one measured in few-layers TiO_2 nanosheets [12] may give information on the average thickness of the crystals grown by thermal treatment: when moving from 146 cm^{-1} (150 °C annealing) to 143 cm^{-1} (300 °C annealing) corresponding thickness is expected to vary from 4 to 7 layers ($\sim 3.8\text{ nm}$ to $\sim 6.7\text{ nm}$, respectively). On the other hand, at higher annealing temperatures, tensile deformation is established, which can lead to the deformation of the TiO_2 octahedra in the O-Ti-O bond, shifting the band towards red values compared to the expected one. Then, plasma also affects the structural properties of thin films, where a decrease in density is associated to an increase of the surface area [13], and thus a formation of low-dimensional materials, as shown for NP. In conclusion, we have shown how the use of plasma during deposition can influence both morphological and structural properties of samples as-grown and annealed. In particular, samples deposited without plasma assistance show more voids on the surface and a lower crystallization temperature than those deposited with plasma. After the annealing treatments, the less dense samples show a blue-shift in RS related to a phonon confinement at the early stage of crystallization; conversely, the denser samples show only a red-shift due to tensile stress at high annealing temperatures.

* * *

The authors are grateful to F. Bobba for his substantial contribution to the results presented, and to all the other members of the Unisa/Unisannio group for scientific discussions. Finally, the authors thank Chemistry and Pharmacy Departments of University of Salerno for allowing the use of X-ray diffractometer and Raman microscope.

REFERENCES

- [1] LAUBE M. *et al.*, *Nucl. Instrum. Methods B*, **113** (1996) 288.
- [2] LEE C. C. *et al.*, *Appl. Opt.*, **44** (2005) 2996.
- [3] DURANTE O. *et al.*, *Nanomaterials*, **11** (2021) 1409.
- [4] COLOMBI P. *et al.*, *Meas. Sci. Technol.*, **20** (2009) 084015.
- [5] TILLACK M. S. *et al.*, *Nanotechnology*, **15** (2004) 390.
- [6] SAMSONOV V. M. *et al.*, *Nanotechnology*, **54** (2009) 526.
- [7] HE H. and SHOESMITH D., *Phys. Chem. Chem. Phys.*, **12** (2010) 8109.
- [8] ALLEN N. S. *et al.*, *Polym. Degrad. Stabil.*, **150** (2018) 31.
- [9] RAJENDER G. and GIRI P. K., *J. Alloy Compd.*, **676** (2016) 591.
- [10] GOLUBOVIĆ A. *et al.*, *J. Sol-Gel Sci. Technol.*, **49** (2009) 311.
- [11] ARORA A. K. *et al.*, *J. Raman Spectrosc.*, **38** (2007) 604.
- [12] ZHANG Y. *et al.*, *Phys. Chem. Chem. Phys.*, **18** (2016) 32178.
- [13] DI FONZO F. *et al.*, *Nanotechnology*, **20** (2016) 015604.